IET Power Electronics

Research Article

IET Journals
The Institution of Engineering and Technology

High-power-factor dimmable LED driver with low-frequency pulse-width modulation

ISSN 1755-4535
Received on 29th August 2015
Revised on 20th March 2016
Accepted on 8th May 2016
doi: 10.1049/iet-pel.2015.0664
www.ietdl.org

Hung-Liang Cheng[1], Yong-Nong Chang[2], Chun-An Cheng[1] ✉, Chien-Hsuan Chang[1], Yu-Hung Lin[1]

[1]*Department of Electrical Engineering, I-Shou University, Kaohsiung, Taiwan*
[2]*Department of Electrical Engineering, Formosa University, Yunlin, Taiwan*
✉ *E-mail: cacheng@isu.edu.tw*

Abstract: A novel dimmable light-emitting diode (LED) driver is proposed in this study. The circuit topology uses two active switches. One active switch shared by a buck–boost converter and a buck converter is operated at high-switching frequency while the other one is low-frequency pulse-width modulated to dim high-power LEDs. The buck–boost converter plays the role of a power-factor corrector. It operates at discontinuous-conduction mode to waveshape the line current to be sinusoidal and in phase with the input-line voltage. The buck converter regulates the dc-link voltage to output a low-frequency pulse-width modulation (PWM) voltage to drive high-brightness LEDs. Since only one power-conversion process is required, and the buck converter works only when the low-frequency PWM voltage is at a high level, the proposed LED driver has the advantage of high efficiency. Besides, it achieves unity power factor and low total current harmonic distortion.

1 Introduction

Owing to the advantages of compact size, long lifetime, high luminous efficiency and fast response, light-emitting diode (LED) has become popularly used as indoor and outdoor lighting sources [1–4]. To comply with the harmonic regulation such as IEC61000-3-2 class C, LED drives with ac sources need to use passive or active power-factor correctors (PFCs) to improve the power factor and reduce the current harmonics at the input line. As compared with passive PFCs that need to use bulky inductors and capacitors, active PFCs have the benefits of small size, low weight and high-power factor within a wide-power range. Hence, the ac-input LED drivers often consist of two power-conversion stages, a PFC stage and a dc/dc stage. Though these two-stage LED drivers possess the benefits of good performance, they require more circuit components and are not cost-effective solutions. Besides, two power-conversion processes would produce more losses, resulting in low circuit efficiency. To overcome these drawbacks, researchers have proposed many single-stage LED drivers by integrating a PFC and a dc/dc converter [5–12].

Generally, the PWM converter such as boost, buck–boost or flyback converter is popularly adopted to serve as the PFC. High-power factor can be achieved by operating them in continuous-conduction mode (CCM), discontinuous-conduction mode (DCM) or critical-conduction mode (CRM). However, in either CCM or CRM operation, it needs to detect the inductor current to waveshape the input current. Also, the switching frequency and duty ratio of the active switch are both inconstant within one input-line cycle. It hinders from obtaining a single-stage solution by integrating a dc/dc converter with a PWM converter that is operated in CCM or CRM. On the contrary, DCM operation has the advantage of simple control. High-power factor can be easily achieved by fixing the switching frequency and duty ratio at constant [13–17]. Though the boost-typed PFC has the simplest circuit structure, yet it has an inherent drawback that the dc-link voltage should be high enough to ensure DCM operation. Generally, the dc-link voltage should be at least twice the peak of the line voltage, resulting in a considerably high-voltage stress on the circuit components [18]. On the contrary, the buck–boost or flyback converters can achieve high-power factor without introducing an excessively high dc-link voltage when they are operated at DCM [7–12]. The flyback converter can provide galvanic isolation and turn ratio to flexibly change the output voltage. However, the leakage inductance of the coupled inductor always produces high-voltage spike when the active switch is turned off.

On the other hand, a dimmable LED driver can adjust the light brightness to provide different lighting effects and meet energy conservation. Dimming methods are divided into two types: the amplitude mode and the low-frequency pulse-width modulation (LFPWM) [19–22]. Both have their advantages and drawbacks. The amplitude mode dimming is more efficient and simple to implement since the LFPWM dimming requires an additional active switch and control circuit to produce square current pulses, resulting in more conducting and switching losses. Drawback to amplitude mode dimming is LED colour shift. Both LED temperature rise and the change of LED current could induce colour shift, and hence reduce the colour rendering index of LED. Contrarily, in LFPWM dimming, LED is turned on and off at a low frequency while the amplitude of LED voltage is maintained at constant. If the LFPWM frequency is high enough, human eyes cannot feel the LED flashes because of the effect of persistence of vision. The average current flowing through the LED can be easily changed by adjusting the duty cycle of the low-frequency pulse, and thus control the LED brightness. Since the level of current flowing through LED is kept constant when the LED is turned on, LED light colour can be consistent.

For a single-stage LED drivers, the input power is controlled either by adjusting the switching frequency or the duty ratio of the shared active switch. Both methods are used to regulate LED voltage (amplitude mode dimming) for dimming operation [7–12]. Since only the shared active switch is used to control the energy transfer between two converters, it is hard to complete PWM dimming. To achieve LFPWM dimming, an extra active switch cascaded in series with the LED string is required. Though this active switch operates at low frequency and has insignificant switching losses, it still produces some conducting losses. In this paper, a dimmable LED driver featuring high-power factor is proposed. It integrates a buck–boost converter and a buck converter. Besides, an LFPWM controlled active switch is embedded to the buck converter. The detail circuit analysis is provided and a prototype circuit was built and tested to verify the accuracy and feasibility of the proposed LED driver.

2 Circuit configuration

Fig. 1 shows an LED driver with the features of high-power factor and dimming capability. It adopts a buck–boost converter to play the role of PFC and a buck converter to further regulate the dc-link voltage to obtain a smooth dc voltage of low ripple to drive LEDs. Metal–oxide–semiconductor field-effect transistors (MOSFETs), S_p and S_b, are operated at a high-switching frequency to serve as the active switches of the buck–boost and the buck converters, respectively. MOSFET S_{pwm} is switched at low frequency to dim the LEDs. It requires three power-conversion processes to drive the LEDs. By integrating the buck–boost and the buck converters and relocating the circuit components, a novel LED driver is proposed, as shown in Fig. 2. The buck–boost converter consists of an inductor L_p, an active switch S_m, diodes D_5 and D_6 and a dc-link capacitor C_{dc}. The buck converter consists of an inductor L_b, active switches S_m and S_{pwm} and diodes D_7 and D_8. It is noted that S_m is shared by both converters. To achieve high-power factor and low total current harmonic distortion (THDi), the buck–boost converter should be designed to operate at DCM. An inductor L_m and a capacitor C_m form a low-pass filter that is used to filter out the high-frequency components of the buck–boost inductor current so that the input-line current can be sinusoidal.

3 Circuit analysis

For simplifying the circuit analysis, the following assumptions are made:

(i) All the circuit components are ideal.
(ii) The capacitance of C_{dc} is large enough, so that the dc-link voltage V_{dc} is considered as a constant voltage source at steady state.
(iii) The capacitance of C_b is large enough and the voltage across it would be constant when S_{pwm} is on.
(iv) The high-switching frequency f_s is much higher than the line frequency f_L. Thus, the sinusoidal input voltage can be considered as constant in each high-switching period.

3.1 Operation modes

At steady state, the proposed LED driver can be separately analysed when the low-frequency active switch S_{pwm} is either on or off. When S_{pwm} is on, the circuit would operate at three different modes in each high-frequency cycle. Fig. 3 shows these operation modes, where the low-pass filter and the diode rectifier (D_1–D_4) are represented by the rectified voltage v_{rec} and the LED string is represented by its equivalent resistance R_{LED}. The theoretical waveforms in each operation mode are shown in Fig. 4.

The ac line-voltage source is given by

$$v_{in}(t) = V_m \sin(2\pi f_L t) \tag{1}$$

where f_L and V_m are the frequency and amplitude of the input-line voltage, respectively. Its rectified voltage can be expressed as

$$v_{rec}(t) = V_m \left|\sin(2\pi f_L t)\right| \tag{2}$$

The detailed circuit analysis for each operation mode is as follows.

3.1.1 Mode I ($t_0 < t < t_1$): Mode I begins at the turn-on instant of S_m. In this mode, there are two current loops as shown in Fig. 3*a*. Since S_m is on, the voltage across the buck–boost inductor L_p is equal to v_{rec}

$$v_p(t) = v_{rec}(t) = V_m \left|\sin(2\pi f_L t)\right| \tag{3}$$

To achieve unity power factor, the buck–boost converter operates at DCM, and hence the inductor current i_p linearly rises from zero. Current i_p can be expressed as follows

$$i_p(t) = \frac{v_{rec}(t)}{L_p}(t - t_0) = \frac{V_m \left|\sin(2\pi f_L t)\right|}{L_p}(t - t_0) \tag{4}$$

Another loop is the inductor current of the buck converter, i_b. It flows through C_{dc}, S_{pwm}, C_b, L_b, S_m and D_7. The voltage across the inductor L_b is equal to

$$v_b(t) = V_{dc} - V_{LED} \tag{5}$$

The buck converter can be designed to operate either at DCM or CCM. The inductor current i_b linearly rises and can be expressed as follows:

$$i_b(t) = i_b(t_0) + \frac{V_{dc} - V_{LED}}{L_b}(t - t_0) \tag{6}$$

Mode I ends at the instant of turning off S_m.

3.1.2 Mode II ($t_1 < t < t_2$): At the beginning of Mod II, i_p reaches a peak value

$$i_{p,peak}(t) = \frac{V_m \left|\sin(2\pi f_L t)\right|}{L_p}(t_1 - t_0) = \frac{V_m \left|\sin(2\pi f_L t)\right|}{L_p} D T_s \tag{7}$$

where D and T_s are the duty ratio and switching period of S_m, respectively. The current i_p diverts from S_m to flow through D_5 and D_6 to charge C_{dc} when S_m is turned off. The voltage across L_p is equal to minus of the dc-link voltage

$$v_p(t) = -V_{dc} \tag{8}$$

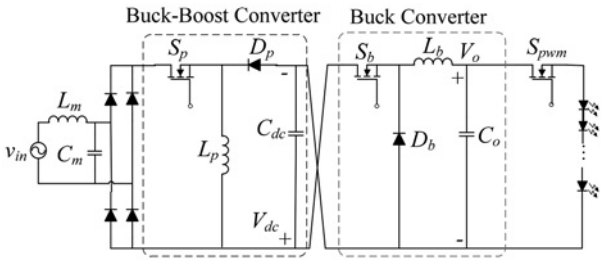

Fig. 1 *LED driver with a buck–boost converter and a buck converter*

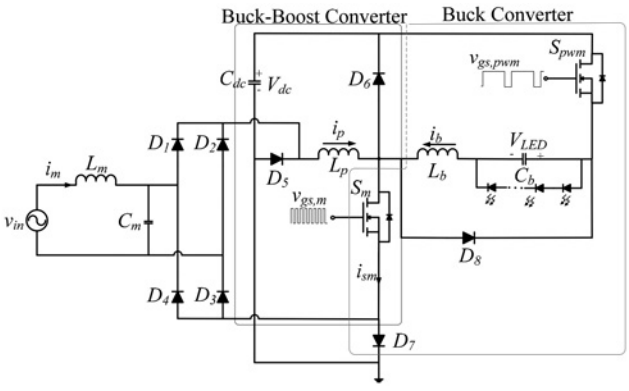

Fig. 2 *Proposed LFPWM dimmed LED driver*

IET Power Electron., 2016, Vol. 9, Iss. 10, pp. 2139–2146

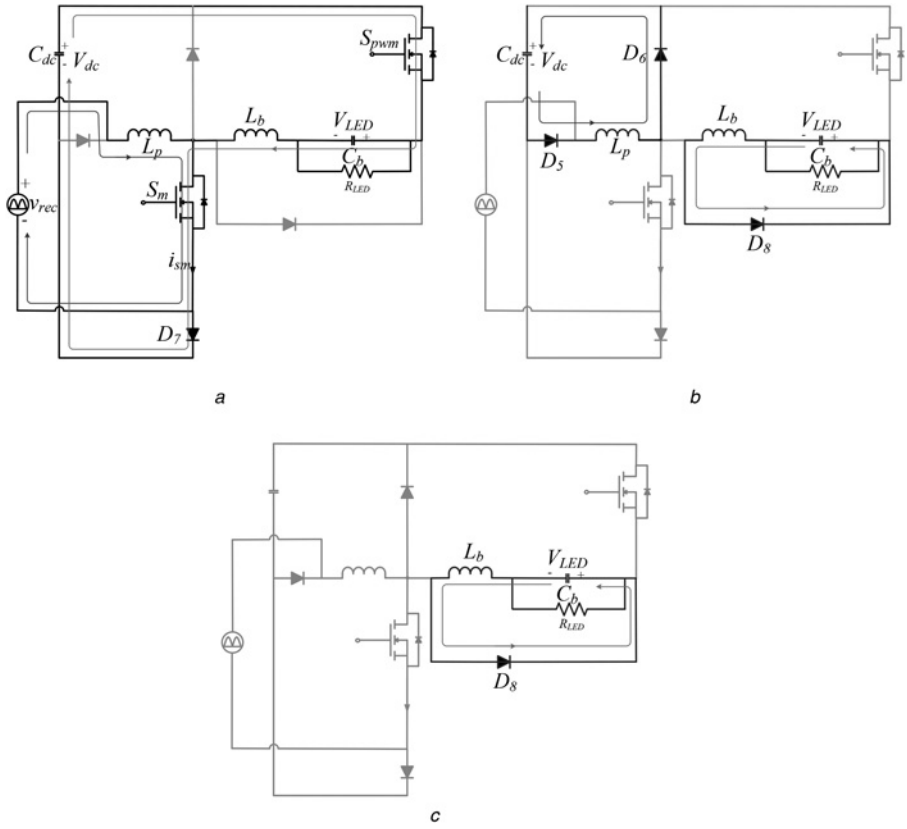

Fig. 3 *Operation modes when S_{pwm} is on*

a Mode I
b Mode II
c Mode III

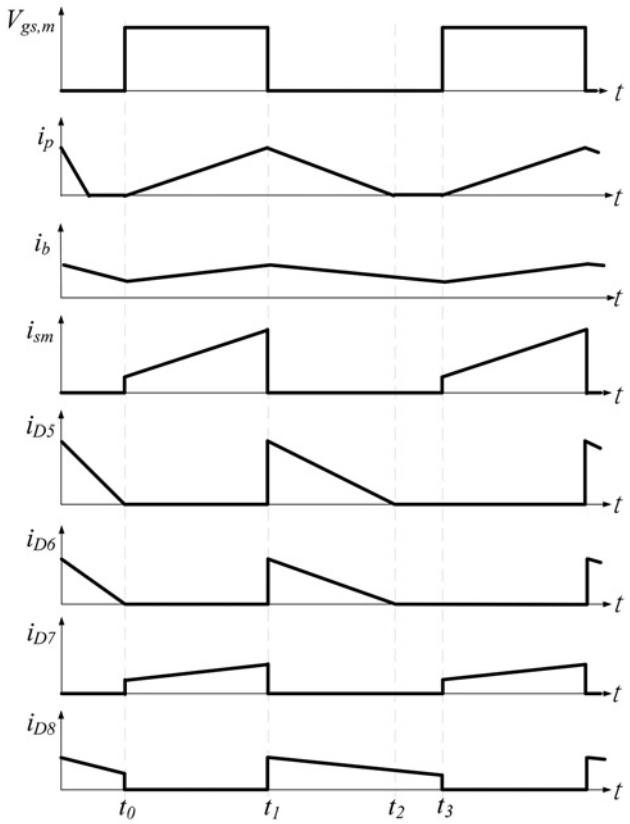

Fig. 4 *Theoretical waveforms when S_{pwm} is on*

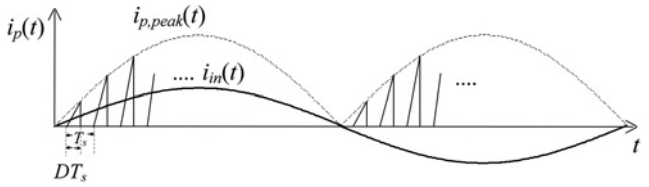

Fig. 5 *Conceptual waveforms of the buck–boost inductor current and the input-line current*

Thereby, current i_p starts to decrease

$$i_p(t) = \frac{V_m\left|\sin\left(2\pi f_L t\right)\right|}{L_p} DT_s - \frac{V_{dc}}{L_p}\left(t - t_1\right) \tag{9}$$

Regarding operation of the buck converter, i_b diverts from S_m to flow through D_8. The voltage across L_b is equal to $-V_{LED}$ and i_b starts to

Table 1 Circuit specifications

Input-line voltage, v_{in}	110 V_{rms} ± 10%, 60 Hz
High-switching frequency, f_s	50 kHz (at rated power operation)
PWM frequency, f_{pwm}	200 Hz
Rated output power, P_{rated}	60 W
Output voltage, V_{LED}	80 V (=4 V × 20)
Output current, I_{LED}	0.75 A
LED equivalent resistance, R_{LED}	106.7 Ω

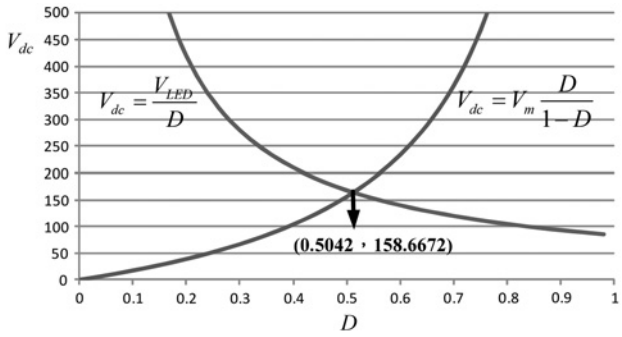

Fig. 6 *V_{dc} against duty ratio of S_m (V_m = 156 V, V_{LED} = 80 V)*

Table 2 Component parameters

Filter inductor L_m	2.0 mH
Filter capacitor C_m	0.47 μF
Buck–boost inductor L_p	0.42 mH
Buck inductor L_b	5.5 mH
DC-link capacitors C_{dc}	200 μF
Buck capacitor C_b	0.47 μF
Active switches S_m, S_{pwm}	IRF840
Diodes D_1–D_4	MUR460
Diodes D_5–D_8	C3D10060A

decrease linearly

$$v_b(t) = -V_{LED} \tag{10}$$

$$i_b(t) = i_b(t_1) - \frac{V_{LED}}{L_b}(t - t_1) \tag{11}$$

When i_p decreases to zero, the circuit enters Mode III.

3.1.3 Mode III ($t_2 < t < t_3$): S_m remains at off state. Current i_p is zero and i_b keeps flowing through D_8 to supply energy to C_b and LEDs. This mode ends at the time when S_m is turned on again and the circuit operation comes back to Mode I of the next high-frequency cycle.

When S_{pwm} is at off stage, the operation modes of the buck–boost converter are the same as those described above. The buck converter is de-energised and the voltage across C_b drops to be lower than the LED cut-in voltage.

According to the discussion of the operation modes, S_m serves as the high-frequency active switch for both converters. Only one power-conversion process is required to drive the LEDs. Besides, the buck converter is energised only when the low-frequency active switch S_{pwm} is on. Therefore, the power loss from the buck converter would be reduced when LEDs are dimmed, leading to further improving the circuit efficiency.

3.2 Buck–boost-typed PFC

Since the switching frequency of the buck–boost converter is much higher than that of the input-line voltage, it is reasonable to consider the rectified input voltage v_{rec} as a constant during a high-frequency

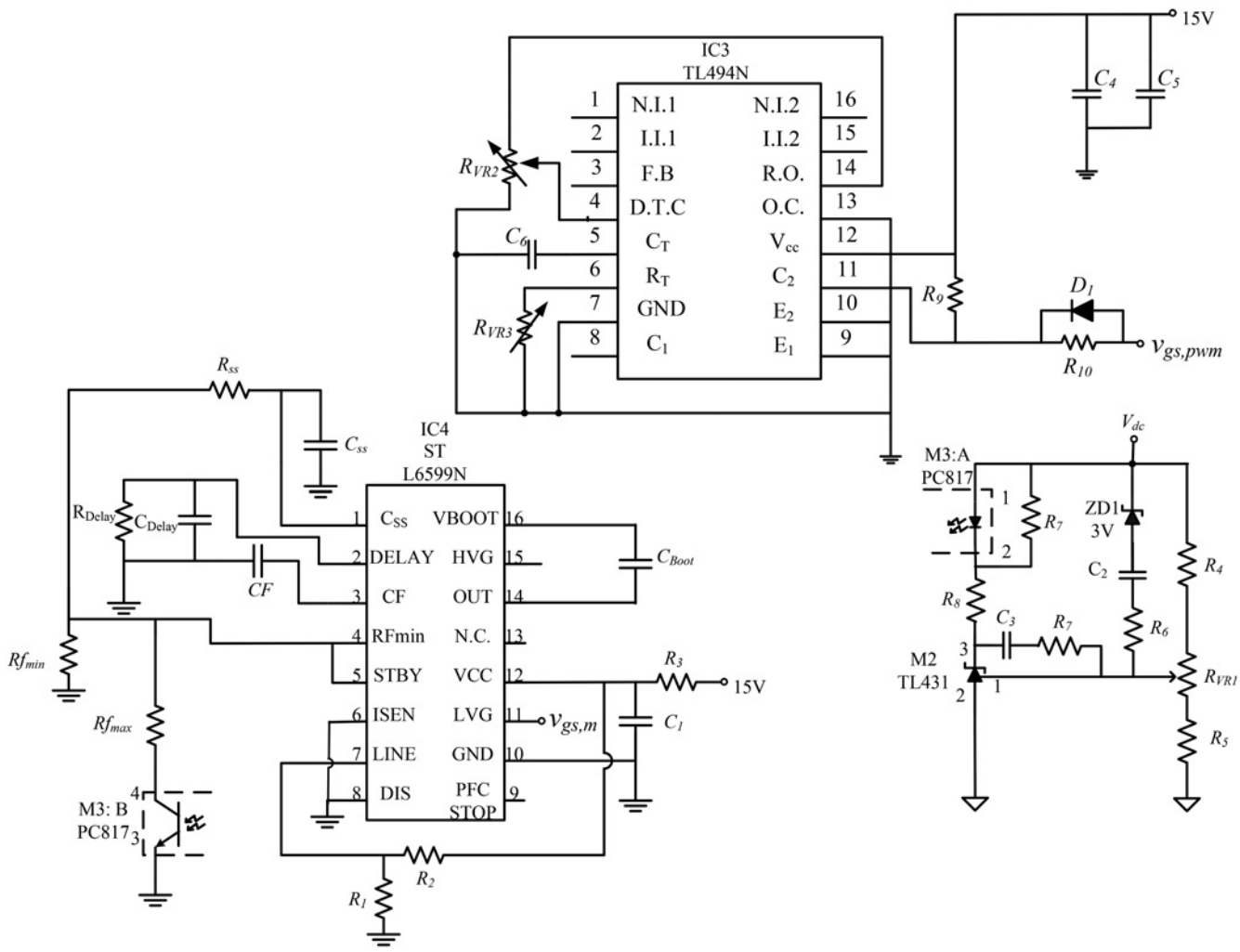

Fig. 7 *Control circuit*

IET Power Electron., 2016, Vol. 9, Iss. 10, pp. 2139–2146

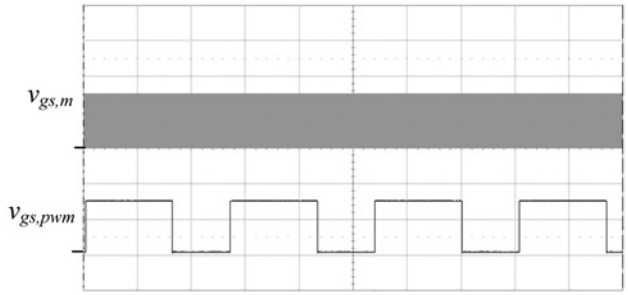

Fig. 8 *Waveforms of $v_{gs,m}$ and $v_{gs,pwm}$ ($v_{gs,m}$, $v_{gs,pwm}$: 10 V/div, time: 2 ms/div)*

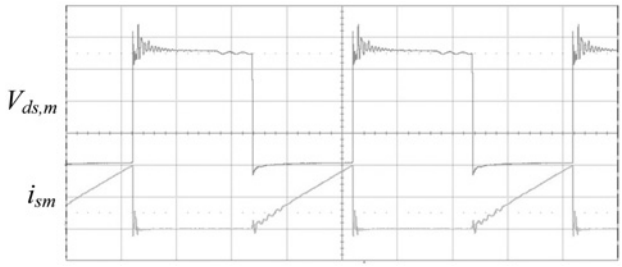

Fig. 9 *Voltage and current waveforms of the high-frequency active switch S_m ($v_{ds,m}$: 100 V/div, i_{sm}: 2 A/div, time: 5 μs/div)*

cycle of the buck–boost converter. From (7), the peak value of the inductor current is proportional to v_{rec}. Fig. 5 shows the conceptual waveforms of the buck–boost inductor current i_p and the input-line current i_{in}. As shown, the peak values of i_p follow a rectified sinusoidal envelope. The current i_{in} is equal to the rising part of i_p and zero elsewhere. By using the low-pass filter (L_m and C_m) to filter out the high-frequency contents of i_p, the current i_{in} will be equal to the average of the rising part of i_p over a high-frequency cycle. The current i_{in} is expressed as follows

$$i_{\text{in}}(t) = \frac{\int_0^{DT_s} i_p(t)\,\mathrm{d}t}{T_s} = \frac{V_m D^2}{2L_p f_s}\sin\left(2\pi f_L t\right) \tag{12}$$

From (12), the input-line current is purely sinusoidal and free of high-frequency harmonics. Besides, it is in phase with the input-line voltage. Theoretically, unity power factor and very low THDi can be achieved. Using (1) and (12), the input power can be obtained by taking an average of the product of the input voltage and the input current over one line-frequency cycle, as follows

$$P_{\text{in}} = \frac{\int_0^{2\pi} v_{\text{in}}(t)\cdot i_{\text{in}}(t)\,d\left(2\pi f_L t\right)}{2\pi} = \frac{V_m^2 D^2}{4L_p f_s} \tag{13}$$

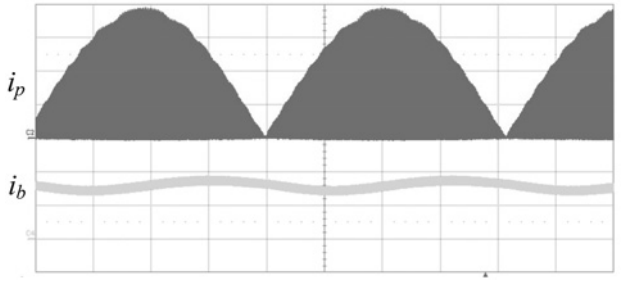

Fig. 10 *Waveforms of i_p and i_b (i_p: 1 A/div, i_b: 0.5 A/div, time: 2 ms/div)*

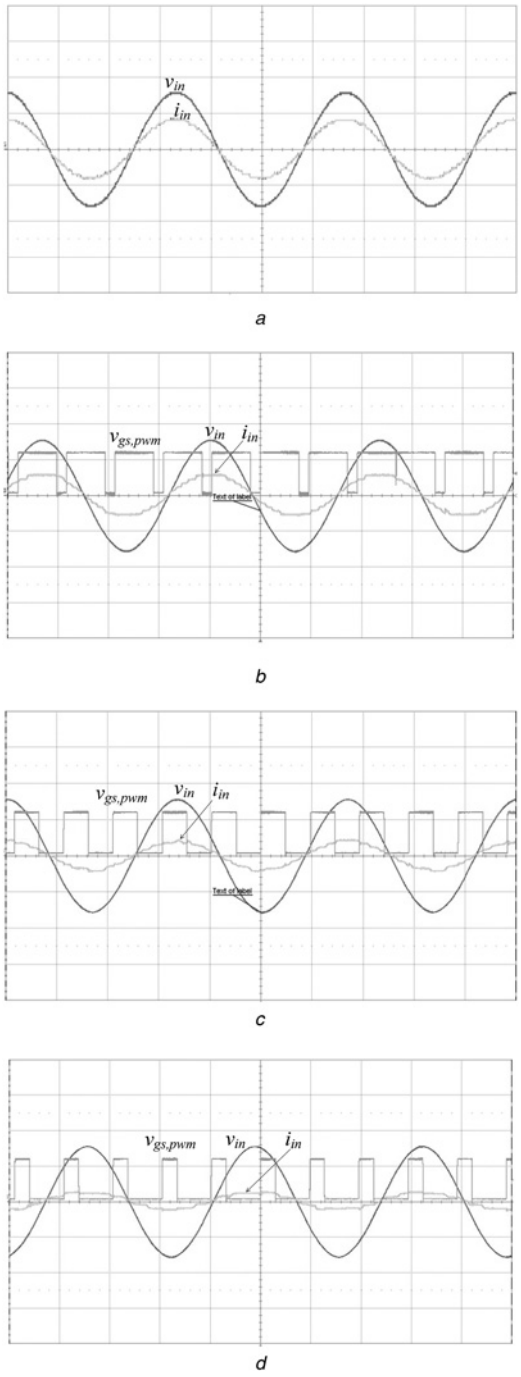

Fig. 11 *Waveforms of v_{in}, i_{in} and $v_{gs,pwm}$ at different dimming values (v_{in}: 50 V/div, i_{in}: 1 A/div, $v_{gs,pwm}$: 10 V/div, time: 5 ms/div)*

a 100% Rated power operation
b 80% Rated power operation
c 50% Rated power operation
d 30% Rated power operation

4 Parameters design and experimental results

A 60 W prototype circuit is illustrated as a design example. The output load is 20 3 W high-brightness LEDs in one string. Table 1 lists the circuit specifications. The ac input voltage is 110 $V_{\text{rms}} \pm 10\%$. The frequencies of S_m and S_{pwm} are 50 kHz and 200 Hz, respectively. The rated voltage and current of the LED are 4 V and 0.75 A. The rated power P_{rated} is 60 W. In this illustrative example, the LEDs are dimmed from 100 to 30% rated power.

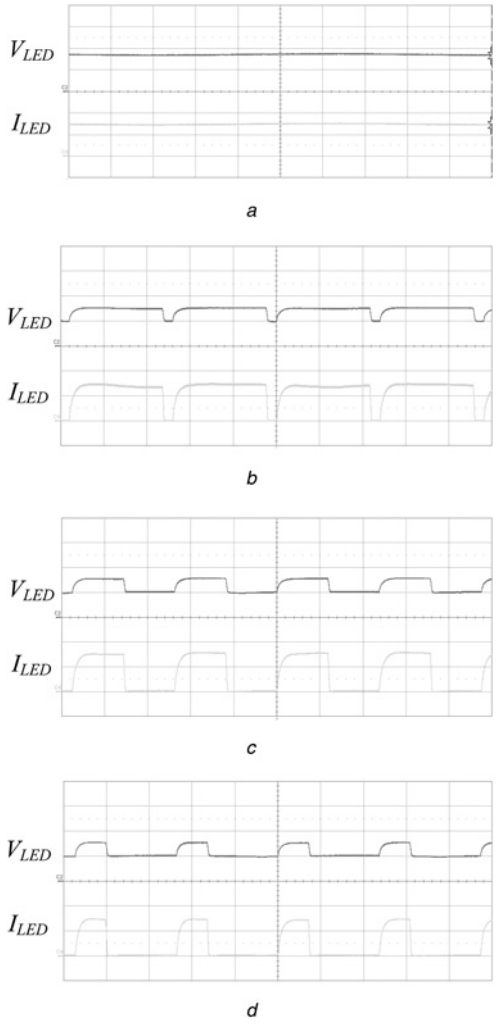

Fig. 12 *Waveforms of V_{LED} and I_{LED} at different duty ratios (V_{LED}: 50 V/div, I_{LED}: 0.5 A/div, time: 2 ms/div)*

a $D_{pwm} = 1.0$
b $D_{pwm} = 0.9$
c $D_{pwm} = 0.5$
d $D_{pwm} = 0.3$

4.1 Parameters design

For DCM operation, V_{dc} should be high enough to ensure that the buck–boost inductor current i_p decreases to zero before turning on S_m. As seen in Fig. 4, i_p decreases from t_1 to t_2. From (9), the duration for i_p decreasing from the peak value to zero is given by

$$t_{off}(t) = t_2 - t_1 = \frac{V_m \left|\sin(2\pi f_L t)\right|}{V_{dc}} DT_s \tag{14}$$

To operate the buck–boost converter at DCM, i_p should decrease to zero before the active switch S_m being turned on. It means that t_{off} must be less than $(1-D)T_s$

$$\frac{V_m \left|\sin(2\pi f_L t)\right|}{V_{dc}} DT_s \le (1-D)T_s \tag{15}$$

From (15), the dc-link voltage should be high enough to meet the inequality

$$V_{dc} \ge V_m \frac{D}{(1-D)} \tag{16}$$

The buck converter is designed to operate at CCM. The relative equation for V_{dc} and V_{LED} is expressed as

$$V_{LED} = DV_{dc} \tag{17}$$

Using (16) and (17), the boundary curves of V_{dc} with respect to the duty ratio of S_m are obtained, as shown in Fig. 6. The duty ratio <0.504 can meet the design requirement. In this illustrative example, the duty ratio and V_{dc} are chosen to be

$$D = 0.48, \quad V_{dc} = 167\,\text{V}.$$

Assuming a circuit efficiency of 90%, L_p is calculated by using (13)

$$L_p = 0.42\,\text{mH}.$$

The current ripple of the buck-inductor current i_b is inversely proportional to inductance of L_b

$$\Delta I_b = \frac{V_{LED}(1-D)T_s}{L_b} \tag{18}$$

At steady-state operation, the average value of i_b is equal to the LED current. Hence, the ripple factor of i_b can be expressed as

$$r_{cur} = \frac{\Delta I_b}{I_b} = \frac{R_{LED}(1-D)T_s}{L_b} \tag{19}$$

For LFPWM dimming, the waveform of LED current should be approximately square. It requires a small buck capacitor C_b for fast charging and discharging. However, small C_b usually complies with high-voltage ripple, resulting in high LED light fluctuation. To reduce the voltage ripple on C_b, the current ripple in the buck inductor L_b should be as low as possible. However, it requires high L_b to obtain low current. Here, 20% ripple factor is designed. Using (19), L_b is calculated

$$L_b = 5.5\,\text{mH}.$$

It is well known that the ripple factor of the output voltage of a buck converter can be expressed as [23]

$$r_{vol} = \Delta V_{LED}/V_{LED} = \frac{(1-D)}{8L_bC_bf_s^2} \tag{20}$$

Using (20) and assuming 1% ripple factor, C_b is calculated

$$C_b = 0.47\,\mu\text{F}.$$

4.2 Experimental results

A prototype circuit was built and tested. Table 2 lists the circuit parameters. Fig. 7 shows the closed-loop control circuit that mainly consists of a PWM controller (TL494N), a double-ended controller (L6599) and a photocoupler (PC817). The TL494N and L6599 output two gated voltages, $v_{gs,pwm}$ and $v_{gs,m}$, to drive the active switches S_{pwm} and S_m, respectively. The variable resistor R_{VR2} is used to adjust the duty ratio of $v_{gs,pwm}$ and the variable resistor R_{VR3} is adjusted to maintain its frequency at 200 Hz. For achieving LFPWM dimming, the output voltage of the buck converter should be kept constant. Since the buck converter is

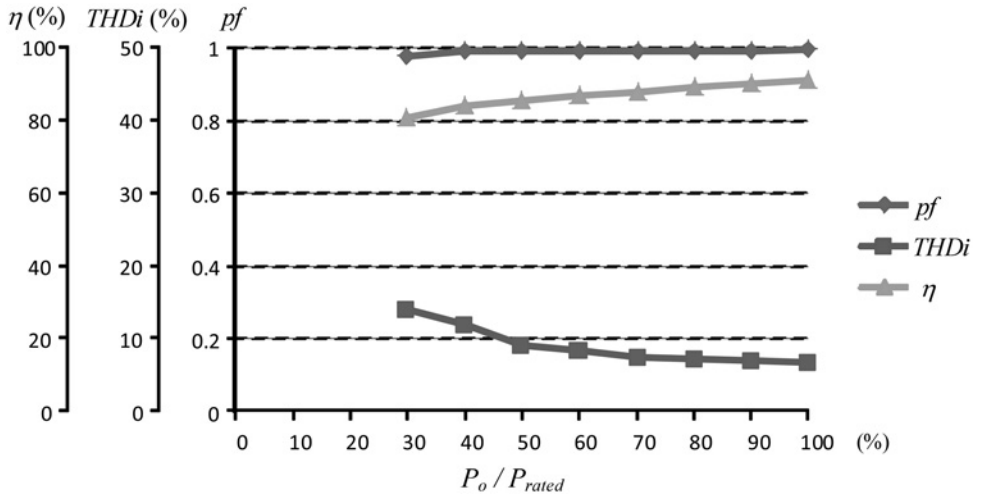

Fig. 13 *Measured power factor, THDi and circuit efficiency for different output powers*

operated at CCM, its output voltage would be constant provided that both the dc-link voltage V_{dc} and the duty ratio of S_m are constant. From (13), the input power is inversely proportional to the high-switching frequency. V_{dc} is sensed and transferred to pin 4 of the L6599 via the phototransistor of the PC817 to modulate the frequency of S_m. By this way, V_{dc} can be maintained at constant while LEDs are dimmed. Fig. 8 shows the waveforms of $v_{gs,m}$ and $v_{gs,pwm}$. The frequency of $v_{gs,pwm}$ is kept at 200 Hz while its duty ratio D_{pwm} is varied from 1 to 0.3 to dim the LEDs. On the contrary, the duty ratio of $v_{gs,m}$ is kept at 0.48 while its frequency is varied to control the input power. Within the dimming range, the frequency of $v_{gs,m}$ will approximately vary from 50 to 167 kHz.

At rated power operation, the duty ratio of $v_{gs,pwm}$ is one. In other words, the active switch S_{pwm} is always on. The measured waveforms at rated power operation are shown in Figs. 9 and 10. Fig. 9 shows the voltage and current waveforms of the high-frequency active switch. The inductor currents of the buck–boost converter and the buck converter are shown in Fig. 10. As shown, the buck–boost converter operates at DCM with the peak values of the inductor current forming a sinusoidal envelope and the buck converter operates at CCM. Dimming operation is achieved by controlling the duty ratio of S_{pwm}. Fig. 11 shows the input voltage and current waveforms at different dimming values. It is noted that the input current is approximately sinusoidal and in phase with the input voltage. At rated power operation, the measured power factor is >0.99 and the THDi is 6.7%. The circuit efficiency is 91%. Fig. 12 shows the waveforms of LED voltage and current at different duty ratios. It shows that the LED voltage and current are well consistent with the design values. The measured LED current ripple is very low. When S_{pwm} is off, it is noted that the LED current drops to zero and LED voltage drops to a certain value which is lower than LED cut-in voltage. The measured values of power factor, THDi and circuit efficiency over a duty-ratio range from 0.3 to 1 are shown in Fig. 13. Within the dimming range, the power factor almost maintains at 0.99, whereas THDi varies from 6.7 to 14.1. Since the output power is inversely proportional to the high-switching frequency, more circuit losses would happen at light load. The circuit efficiency drops to 0.81 at 30% rated power. By the control scheme of LFPWM, LED can be easily and effectively dimmed.

5 Conclusions

An LFPWM dimmed LED driver is proposed by integrating a buck–boost converter and a buck converter. Besides, an active switch is embedded to perform the dimming operation. The buck–boost converter plays the role of PFC and is operated at DCM to achieve a high-power factor and low THDi. The buck converter is both high-frequency and low-frequency modulated to provide a low-frequency pulsed voltage to drive 20 high-brightness LEDs. Only one power-conversion process is required to drive LEDs, leading high circuit efficiency. The circuit operation is described and design equations are derived. A 60 W prototype circuit was built and measured. The experimental results of high circuit efficiency (91%), high-power factor (0.99), low THDi (6.7%) and low LED current ripple (3%) demonstrate the feasibility of the proposed LED driver. Also, the LEDs can be effectively dimmed by the control scheme of LFPWM.

7 References

1 Kim, H.C., Yoon, C.S., Ju, H., *et al.*: 'An ac-powered, flicker-free, multi-channel LED driver with current-balancing SIMO buck topology for large area lighting applications'. Proc. IEEE Applied Power Electronic Conf., 2014, pp. 3337–3341
2 Ma, H., Zheng, C., Yu, W., *et al.*: 'Bridgeless electrolytic capacitor-less valley-fill AC/DC converter for offline twin-bus light-emitting diode lighting application', *IET Power Electron.*, 2013, **6**, (6), pp. 1132–1141
3 Wang, C.C., Wu, K.H., Liu, Y.C., *et al.*: 'Study and implementation of an improved-power factor alternating-current-light emitting diode driver', *IET Power Electron.*, 2015, **8**, (7), pp. 1156–1163
4 Chen, C.C., Wu, C.Y., Chen, Y.M., *et al.*: 'Sequential color LED backlight driving system for LCD panels', *IEEE Trans. Power Electron.*, 2007, **22**, (3), pp. 919–925
5 Xie, X., Wang, J., Zhao, C., *et al.*: 'A novel output current estimation and regulation circuit for primary side controlled high power factor single-stage flyback LED driver', *IEEE Trans. Power Electron.*, 2012, **27**, (11), pp. 4602–4612
6 Hsieh, Y.T., Liu, B.D., Wu, J.F., *et al.*: 'A high-dimming-ratio LED driver for LCD backlights', *IEEE Trans. Power Electron.*, 2012, **27**, (11), pp. 4562–4570
7 Li, Y.C., Chen, C.L.: 'A novel primary-side regulation scheme for single-stage high-power-factor AC–DC LED driving circuit', *IEEE Trans. Ind. Electron.*, 2013, **60**, (11), pp. 4978–4986
8 Alonso, J.M., Antonio, J.C., David, G., *et al.*: 'High-power-factor light-emitting diode lamp power supply without electrolytic capacitors for high-pressure-sodium lamp retrofit applications', *IET Power Electron.*, 2013, **6**, (8), pp. 1502–1515
9 Alonso, J.M., Viña, J., Vaquero, D.G., *et al.*: 'Analysis and design of the integrated double buck–boost converter as a high-power-factor driver for power-LED lamps', *IEEE Trans. Ind. Electron.*, 2012, **59**, (4), pp. 1689–1697
10 Cheng, C.A., Cheng, H.L., Yang, F.L., *et al.*: 'Single-stage driver for supplying high-power light-emitting-diodes with universal utility-line input voltages', *IET Power Electron.*, 2012, **5**, (9), pp. 1614–1623
11 Li, Y.C., Chen, C.L.: 'A novel single-stage high-power-factor AC-to-DC LED driving circuit with leakage inductance energy recycling', *IEEE Trans. Ind. Electron.*, 2012, **59**, (2), pp. 793–802
12 Hwu, K.I., Tu, W.C., Lai, C.Y.: 'Light-emitting diode driver with low-frequency ripple suppressed and dimming efficiency improved', *IET Power Electron.*, 2014, **7**, (1), pp. 105–113
13 Arias, M., Lamar, D.G., Linera, F.F., *et al.*: 'Design of a soft-switching asymmetrical half-bridge converter as second stage of an LED driver for street lighting application', *IEEE Trans. Power Electron.*, 2012, **27**, (3), pp. 1608–1621
14 Athalye, P., Harris, M., Negley, G.: 'A two-stage LED driver for high-performance high voltage LED fixtures'. Proc. IEEE Applied Power Electronic Conf., 2012, pp. 2385–2391
15 Aguilar, D., Henze, C.P.: 'LED driver circuit with inherent PFC'. Proc. IEEE Applied Power Electronic Conf., February 2010, pp. 605–610

16 Lohaus, L., Rossius, A., Sturm, A., *et al*.: 'An efficient dual-stage power supply topology for series connected control devices in intelligent lighting systems'. Proc. IEEE Energy Conversion Congress and Exposition (ECCE), 2015, pp. 2454–2460
17 Singh, B., Singh, B.N., Chandra, A., *et al*.: 'A review of single-phase improved power quality AC–DC converters', *IEEE Trans. Ind. Electron.*, 2003, **50**, (5), pp. 962–981
18 Liu, K.H., Lin, Y.L.: 'Current waveform distortion in power factor correction circuits employing discontinuous-mode boost converters'. Proc. IEEE Power Electronics Specialists Conf., 1989, pp. 825–829
19 Lun, W.K., Loo, K.H., Tan, S.C., *et al*.: 'Bilevel current driving technique for LEDs', *IEEE Trans. Power Electron.*, 2009, **24**, (12), pp. 2920–2932
20 Hong, S., Kim, H., Park, J., *et al*.: 'Secondary-side LLC resonant controller IC with dynamic PWM dimming and dual-slope clock generator for LED backlight units', *IEEE Trans. Power Electron.*, 2011, **26**, (11), pp. 3410–3422
21 Chiu, H.J., Lo, Y.K., Chen, J.T., *et al*.: 'A high-efficiency dimmable LED driver for low-power lighting applications', *IEEE Trans. Ind. Electron.*, 2010, **57**, (2), pp. 735–743
22 Lin, M.S., Chen, C.L.: 'An LED driver with pulse current driving technique', *IEEE Trans. Power Electron.*, 2012, **27**, (11), pp. 4594–4601
23 Batarseh, I.: 'Power electronic circuits' (Wiley, Hoboken, NJ, 2004)